

# The mechanical properties of PVC under high pressure

J. YUAN, A. HILTNER, E. BAER

*Department of Macromolecular Science, Case Institute of Technology,  
Case Western Reserve University, Cleveland, Ohio 44106, USA*

The deformation properties of PVC have been studied under high pressure. Craze initiation and yield criteria have been proposed. The brittle-to-ductile transition was observed between  $1 \times 10^7$  and  $2 \times 10^7$  Pa, which is a relatively low transition pressure compared to polystyrene. Deformation in the post-yield region occurred by neck formation and subsequent drawing to produce chain orientation. When PVC was exposed to the pressure-transmitting fluid, silicon oil, a strong environmental stress cracking effect was observed.

## 1. Introduction

During the past two decades, the effects of the superposition of hydrostatic pressure on the mechanical properties of polymers have been extensively investigated. As a result of these studies a much deeper understanding of deformation and fracture processes has been provided which could not be achieved by experiments conducted at atmospheric pressure. Under pressure a transitional change in the fracture mode from brittle to ductile has been reported for a few amorphous polymers including polystyrene (PS) [1-4], poly(methyl methacrylate) (PMMA) [5], and polyimide (PI) [6]. These polymers, which behave in a brittle manner at atmospheric pressure, become ductile when extended under high pressure. The nature of this brittle-to-ductile transition has been studied by Matsushige *et al.* [1, 5] who suggested the existence of competing micro-deformation processes of crazing and shear banding which have different pressure dependencies.

More recently, Baer and his co-workers [1, 5, 7-9] have reported that the conventional "inert" pressurizing fluid such as silicon oil has a large environmental effect on the tensile properties of amorphous polymers when studied under high pressure. PS has been reported to undergo a brittle-to-ductile transition at pressures between  $2.9 \times 10^8$  and  $3.0 \times 10^8$  Pa (2.9 and 3.0 kbar) when exposed to the pressure transmitting fluid; however, this brittle-to-ductile transition shifts to

much lower pressures between  $3 \times 10^7$  and  $4 \times 10^7$  Pa if the environmental effect due to the pressure-transmitting fluid is prevented. A similar pressure-induced environmental effect has also been found in the study of PMMA [5]. No brittle-to-ductile transition could be observed up to  $4 \times 10^8$  Pa when the test specimen was exposed to the pressurizing liquid. However, again a distinct brittle-to-ductile transition was observed between  $2 \times 10^7$  and  $3 \times 10^7$  Pa when the test samples were shielded from the pressure-transmitting fluid. Further studies using Fourier transform infrared (FTIR) have shown that the pressure-transmitting fluid penetrates into the polymer under tension up to the edge of the crazing zone and the penetration coefficient depends on the viscosity of the pressurizing fluid as well as the superimposed hydrostatic pressure.

The yield stress has been reported to increase significantly with hydrostatic pressure, and the classical Tresca and von Mises yield criteria no longer describe the material behaviour since both yield criteria predict a pressure independent yield stress [10]. Several attempts have been made in order to modify these criteria to account for the large pressure dependence of yield stress observed in polymeric materials. One of the most successful yield criteria is the linear pressure modified von Mises yield criterion [11-13], which suggests that the stress deviator required for the critical distortional strain array energy is dependent on the

mean stress. Another linear pressure-dependent yield criterion is the Mohr–Coulomb yield criterion [14–16], which was originally applied to soils, implying that the maximum shear stress required for yielding depends on the normal stress component of the shear plane. Raghava *et al.* [17] have proposed a nonlinear pressure modified von Mises yield criterion which requires the knowledge of the compression and tensile yield stress at atmospheric pressure. Recently, Li and Wu [18] have suggested a three-parameter yield criterion, clarifying the differentiation between the effects of mean stress and the normal stress component to the shear plane.

Sternstein *et al.* [12, 13, 19] first introduced the concept of a craze initiation criterion based on the studies in biaxial stress fields such as tension–tension and torsion–tension. A similar craze initiation criterion in terms of critical strain instead of critical stress has also been suggested by Oxborough and Bowden [20] from biaxial compression–tension experiment. However, both craze initiation criteria require a positive first stress invariant which could not satisfy the recent experimental observations [1, 21–23]. A quite different type craze initiation criterion has been proposed by Gent [24] who hypothesized that the craze formation is a process of a transformation from a glassy state to a soft rubbery state at the flow tip, followed by the cavitation of the rubbery phase under dilatant stress. Most recently, Moet *et al.* [25] using new experimental findings have proposed that crazing occurs as the maximum normal stress at the surface flaw tip reaches a critical value.

The tensile modulus of polymers has also been reported to increase with the hydrostatic pressure. To account for the pressure dependence of the modulus Aibinder *et al.* [26] have introduced a linear relationship between modulus and pressure based on the finite elasticity theory. Later, Sauer *et al.* [27–30] proposed a similar linear relationship which predicts a higher pressure coefficient value. A more complicated nonlinear pressure-dependent relation has also been suggested by Matsushige *et al.* [5] in order to predict the pressure dependence of the modulus in PMMA.

The purpose of this work was to study the mechanical properties of non-plasticized poly(vinyl chloride) (PVC) under pressure, to elucidate the brittle-to-ductile transition and the possible mechanism for this transition. In addition,

the environmental effects due to the pressure-transmitting fluid on the tensile properties and on the brittle-to-ductile transition was examined, as well as the criteria of craze initiation and shear yielding.

## 2. Experimental details

### 2.1. Materials

The material used in this study was PVC supplied by the F.F. Goodrich Company in a form of 1.27 cm × 1.27 cm × 12.7 cm rod prepared from two PVC resins, Geon 110 × 346 (average weight molar mass,  $M_w = 1.0 \times 10^5$ ,  $M_w/M_n = 2.7$ , where  $M_n$  is the average number molar mass) and Geon 103EP ( $M_w = 2.0 \times 10^5$ ,  $M_w/M_n = 2.1$ ). The rods contained 2 wt % Thermolite T-31 stabilizer (dibutyltin bis(octyl thioglycolate) supplied by M.T. Chemicals and were compression-moulded at 210°C. Tensile specimens were machined from the compression-moulded rods into a cylindrical geometry specially designed for our high pressure testing machine, as described in a previous publication [1]. A slight modification of the fillet part (0.25"R) allowed for better machining of the sample. In order to prevent the possible environmental effect due to the pressure-transmitting fluid, the gauge section of specimens was sealed with Teflon tape and transparent silicon rubber.

### 2.2. Tensile measurements

The apparatus used in this study of tensile behaviour under superimposed hydrostatic pressure is essentially a constant crosshead speed testing machine. Tensile measurements for both sealed and unsealed specimens were conducted at a strain rate of approximately 10% min<sup>-1</sup> and at a temperature of 76 ± 2°F. During specimen straining a constant pressure was maintained. Silicon oil (Dow Corning 200 Fluids, 500 C. St.) was used as a pressure-transmitting fluid. Tensile measurements at atmospheric pressure were performed in an Instron testing machine.

## 3. Results and discussion

### 3.1. Stress and strain behaviour

Tensile measurements under hydrostatic pressure were performed for both sealed and unsealed specimens at pressures up to 3 × 10<sup>8</sup> Pa. Fig. 1 shows nominal tensile stress–strain curves for sealed samples at various pressures. The points showing deviation from linearity indicated by arrows X and Y correspond to the craze initiation

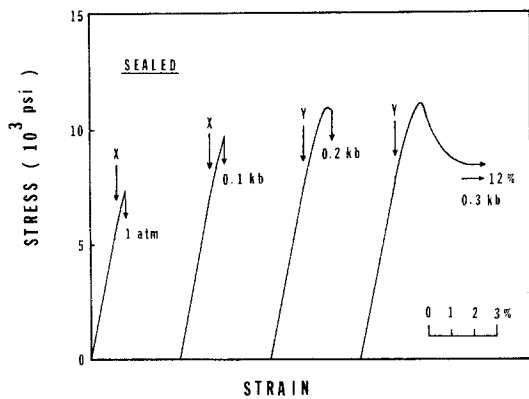


Figure 1 Stress-strain curves of sealed specimens at various pressures. Deviation points indicated by arrows X and Y correspond to craze initiation and shear band initiation points, respectively. (1 kbar =  $10^8$  Pa.)

and shear band initiation. It is noted that the brittle fracture stress increases substantially as the pressure increases from atmospheric pressure to  $1 \times 10^7$  Pa. A brittle-to-ductile transition was observed at the pressure between  $1 \times 10^7$  and  $2 \times 10^7$  Pa. Herein, we define the term "brittle" as specimen fracture at a relatively low strain level prior to the onset of any upper shear yielding, while "ductile" corresponds to specimen fracture after upper shear yielding. At the transition pressure, upper shear yielding occurred and the ultimate engineering strain increased with increasing pressure. The yield stress was also observed to increase with pressure to a lesser extent when compared with the pressure dependency of the brittle fracture stress. Pae and Sauer [30] have conducted a similar study on the plasticized PVC. The pressure-transmitting fluid was a kerosene-oil mixture, and under these conditions the polymer, which was highly ductile at atmospheric pressure, became less ductile at  $2.76 \times 10^8$  Pa and then again increased its ductility at pressures up to  $6.89 \times 10^8$  Pa. This ductile-less ductile-ductile phenomenon was explained by the presence of a brittle-to-ductile transition at about  $2.76 \times 10^8$  Pa, which is much higher than the brittle-to-ductile transition observed in this work and undoubtedly could be as a result of an environmental effect due to the pressure-transmitting fluid.

The effect of the environment is shown in Fig. 2 for unsealed specimens at various pressures. Craze initiation could be observed up to  $2 \times 10^7$  Pa. At higher pressures fracture in a more brittle manner was observed at lower strain levels without

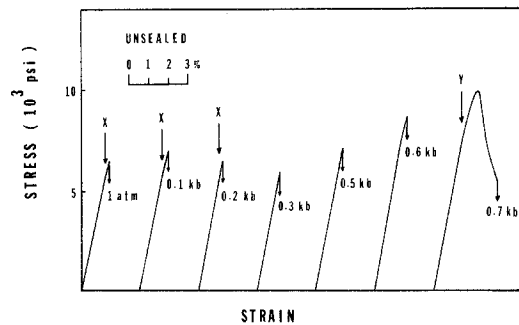


Figure 2 Stress-strain curves of unsealed specimens at various pressures. Deviation points indicated by arrows X and Y correspond to craze initiation and shear band initiation points, respectively.

craze formation. The brittle-to-ductile transition occurred at a higher pressure between  $6 \times 10^7$  and  $7 \times 10^7$  Pa and undoubtedly reflects the environmental effect due to the silicon oil.

### 3.2. Environmental effect

In Fig. 3 the tensile stress and strain behaviour for both sealed and unsealed tests conducted at atmospheric pressure and at  $5 \times 10^7$  Pa are compared. At atmospheric pressure, a very small (if any) environmental effect on the fracture behaviour was observed. In contrast, a large environmental effect due to the pressure-transmitting fluid was observed at  $5 \times 10^7$  Pa. At this pressure, the sealed specimen showed very ductile behaviour while the specimen tested in the silicon oil fractured in a brittle manner at a very low strain level. This pressure induced environmental effect is expected due to the increase in the driving force for transport of silicon oil into PVC as the hydrostatic pressure is increased. A similar pressure-induced environ-

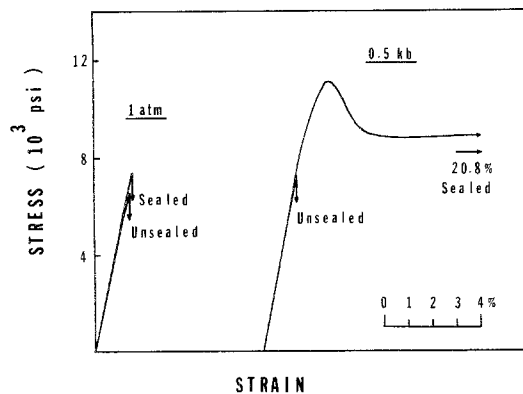


Figure 3 Stress-strain curves of sealed and unsealed specimens at 1 atm and 0.5 kbar ( $5 \times 10^7$  Pa.)

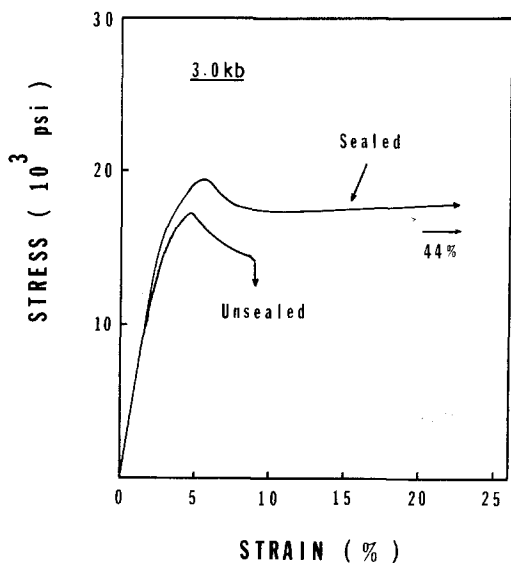


Figure 4 Stress-strain curves of sealed and unsealed specimens at 3.0 kbar. ( $3 \times 10^8$  Pa.)

mental effect has been reported by Baer and co-workers [1, 5, 7, 8] for PS and PMMA. However, at very high pressures, where both sealed and unsealed specimens became ductile, no significant environmental effect due to silicon oil on the tensile yield stress was observed for PS. In contrast, the tensile yield stress of PVC was lowered by the silicon oil at  $3 \times 10^8$  Pa as is shown in Fig. 4. This lowering in the yield stress of PVC is probably due to the plasticization of PVC by silicon oil under high pressure.

Fig. 5 shows the pressure dependencies of brittle fracture stress and upper shear yield stress for both sealed and unsealed behaviour. It is noted that the environmental effect due to the pressure-transmitting fluid is operative over the entire range of test pressures. Environmental stress cracking occurred at the pressures between  $2$  and  $6 \times 10^7$  Pa. The pressure-dependent driving force for the transport of the silicon oil into the PVC is opposed by the densification of the polymer by the hydrostatic pressure [31, 32]. The differences in the yield stresses for the sealed and unsealed samples, as in Fig. 4, could be a result of the plasticization of PVC by silicon oil under high pressure.

### 3.3. Pressure dependence of the modulus

Young's modulus for polymers has been reported to increase substantially with increasing hydrostatic pressure. In order to predict the pressure

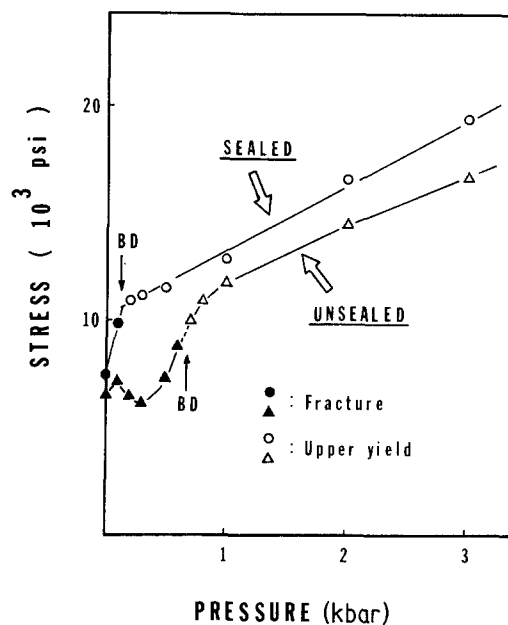


Figure 5 The effects of hydrostatic pressure on fracture and yield stresses in sealed and unsealed specimens. Arrows BD indicate the brittle-to-ductile transition.

dependency of the modulus Aibinder *et al.* [26] suggested a linear relationship between modulus and pressure based on finite elasticity theory derived by Murnaghan [33] and further developed by Birch [34].

$$E(p) = E_0 + 2(5 - 4\nu)P \quad (1)$$

where  $E(P)$  and  $E_0$  are Young's moduli at pressure  $P$  and at atmospheric pressure, respectively, and  $\nu$  is Poisson's ratio. However, this equation did not fit with their experimental results. A similar relation derived from the same reference with slightly different assumptions was proposed by Sauer and co-workers [27-30] who reported that experimental data agreed well with predicted values for polycarbonate (PC) and polytetrafluoroethylene (PTFE) at least in the low pressure region. The equation used was

$$E(p) = E_0 + mp \quad (2)$$

where  $m$  is a function only of Poisson's ratio,  $M = 2(5 - 4\nu)(1 - \nu)$ .

Fig. 6 shows a nearly linear dependency of the modulus for PVC up to  $3 \times 10^8$  Pa. From a physical point of view, this pressure effect on the modulus can be understood by considering the reduction of the excess free volume which is related to the increase of the glass transition with pressure [35]. The slope calculated from the best

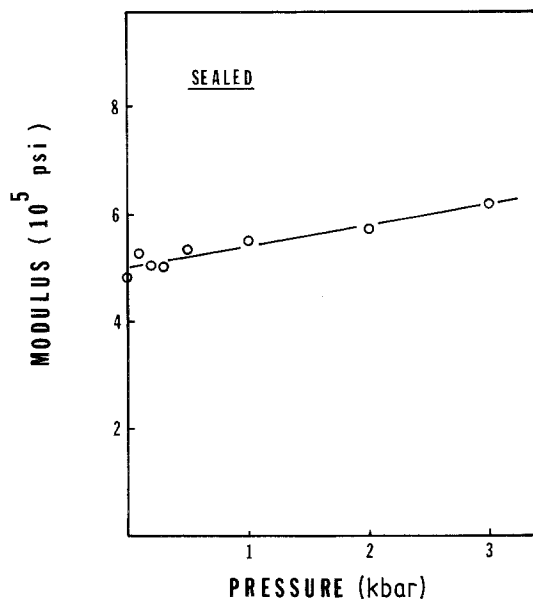


Figure 6 Pressure dependency of modulus for sealed specimens.

fit of linear least squares is about 0.27 which is lower than the value 0.41 predicted from the relation suggested by Sauer using Poisson's ratio of 0.40 [36], and much lower than that predicted from Ainsbinder's correlation. It would be instructive to measure Poisson's ratio under pressure instead of using the value taken at atmospheric pressure. The calculated Poisson's ratio from our experimental data using Sauer's equation is about 0.53, which seems unreasonably high. It is noted that in the literature the pressure coefficient of the modulus reported for one polymer was almost twice as large as another polymer although both materials have the same reported Poisson's ratio [30]. Therefore, further investigations using parameters in addition to Poisson's ratio have to be undertaken in order to predict the pressure dependency of the modulus.

### 3.4. Brittle-to-ductile transition

Fig. 7 shows the pressure dependencies of craze initiation stress and shear band initiation stress in addition to brittle fracture and upper shear yield stresses. Both craze and shear band initiation stresses increase with increasing pressure. It is noted that the craze initiation stress is more pressure-sensitive than the shear band initiation stress. This is due to the fact that crazing is essentially a dilational void forming process while the shear band initiation requires little volume change.

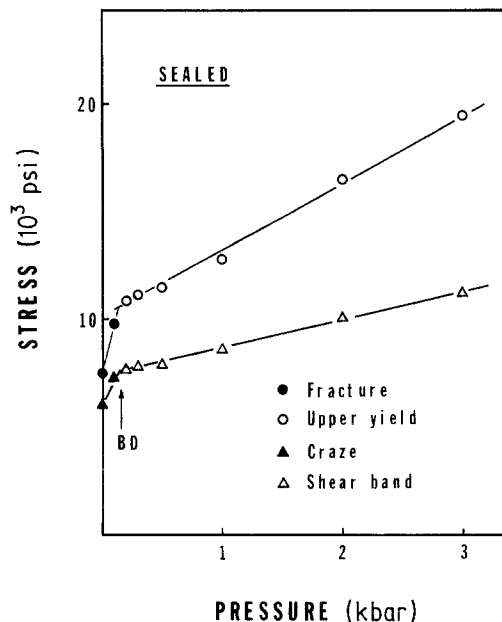


Figure 7 The effects of hydrostatic pressure on the fracture, upper yield, craze initiation, and shear band initiation stresses for sealed specimens. Arrow BD indicates the brittle-to-ductile transition.

The brittle-to-ductile transition indicated by the arrow BD occurred at the pressure where the craze and shear band initiation curves intersect. Above this transition pressure, shear bands initiate at a lower stress level than crazes thus preventing crazing which is responsible for fracture at low strain levels.

### 3.5. Pressure dependence of craze initiation

It is reasonable to observe that the craze initiation stress increases with pressure due to the fact that crazing is essentially a dilational process involving voids formation which is suppressed by pressure. Although Hoare and Hull [37] have reported that a few localized crazes could form at the specimen surface at lower stress levels than that corresponding to the inflection point on the stress-strain curve, a more recent study under creep conditions showed that intense crazing occurs only when deviation from linearity occurs. Fig. 8 shows the effect of pressure on the craze initiation stress for sealed and unsealed specimens. The craze initiation stress for unsealed samples is less pressure dependent, and this is similar to the observations of Matsushige *et al.* [1, 5] on PS and PMMA. In order to account for the difference between the sealed and unsealed experiments, Moet *et al.* [25] have proposed a craze initiation criterion which suggests

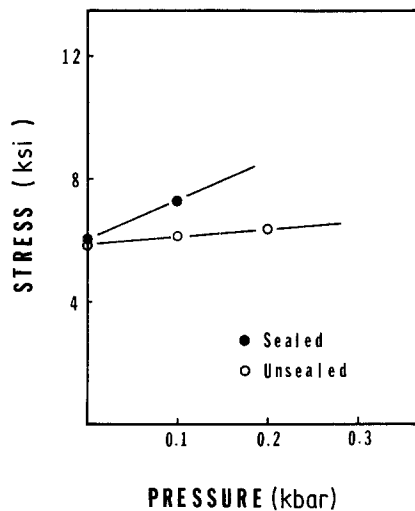


Figure 8 Pressure dependencies of craze initiation stress for sealed and unsealed specimens.

that crazing occurs as the maximum normal stress at the surface flaw tip reaches a critical value.

### 3.6. Yield behaviour

In general, two types of yield criteria have been used to describe the yield behaviour in materials: (1) the critical distortional strain energy, and (2) the critical shear stress conditions [10]. Such classical one-parameter yield criteria, which predict a pressure independent yield stress, cannot describe the pressure dependence of the yield behaviour in polymers such as those shown in Fig. 7.

The classical von Mises yield criterion is based on the assumption that no volume change occurs at yield and thus only the stress deviators provide contributions to the distortional strain energy. Recognizing the fact that yielding in polymers is associated with relatively large volume changes, the octahedral strain which is in directions normal to the planes of the octahedron can no longer be zero. Subsequently, one must take into account the contributions of both the octahedral normal and octahedral shear stresses in order to predict the yield behaviour. A more general form of the von Mises yield criterion has been previously proposed [11–13] to take into account the pressure dependency:

$$\tau_{\text{oct}} + \mu\sigma_{\text{oct}} = K_{\text{oct}} \quad (3)$$

where  $\tau_{\text{oct}} = 1/3[(\sigma_1 - \sigma_2)^2 + (\sigma_2 - \sigma_3)^2 + (\sigma_3 - \sigma_1)^2]^{1/2}$  is the octahedral shear stress,  $\sigma_{\text{oct}} = 1/3(\sigma_1 + \sigma_2 + \sigma_3)$  is the octahedral normal stress,  $K_{\text{oct}}$  is a constant, and  $\mu$  the octahedral normal

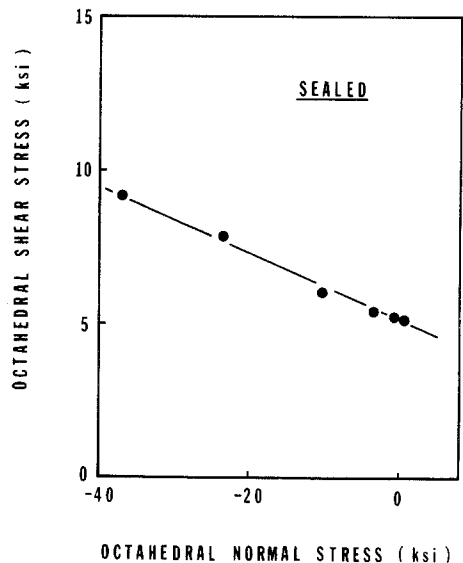


Figure 9 Upper yielding of sealed specimens expressed as octahedral shear stress against hydrostatic stress.

stress coefficient. In the case of plastic distortion in pure shear,  $\mu = 0$  and  $\tau_{\text{oct}} = K_{\text{oct}}$ . Fig. 9 shows the plot of octahedral shear stress against octahedral normal stress for PVC. It is noted that this form of the von Mises yield criterion fits our experimental data. Values of  $K_{\text{oct}}$  and  $\mu$  calculated from the best linear least squares are  $3.53 \times 10^7$  Pa and 0.11, respectively. As is shown in Table I, the results agree well with the data from biaxial compression–tension studies on PVC reported by Bowden and Jukes [38].

An attempt has also been made to check the validity of the Mohr–Coulomb yield criterion [14–16], in which the maximum shear stress is dependent on the normal stress to the shear plane as given by

$$\tau_{\text{max}} + \alpha\sigma_n = K_{\text{max}} \quad (4)$$

where  $\tau_{\text{max}}$  is the maximum shear stress,  $\sigma_n$  the normal stress to the shear plane,  $K_{\text{max}}$  the maximum shear stress in pure shear, and  $\alpha$  the normal stress coefficient. Fig. 10 shows the construction of Mohr circles corresponding to the upper shear yield, and the common tangent line indicating the maximum shear stress. It is not surprising that the Mohr–Coulomb yield criterion also describes adequately the experimental observations. Values

TABLE I

$K_{\text{oct}}$ ( $10^7$ Pa)	$\mu$	Reference
3.53	0.11	
3.43 ( $\pm 0.12$ )	0.11 ( $\pm 0.02$ )	[38]

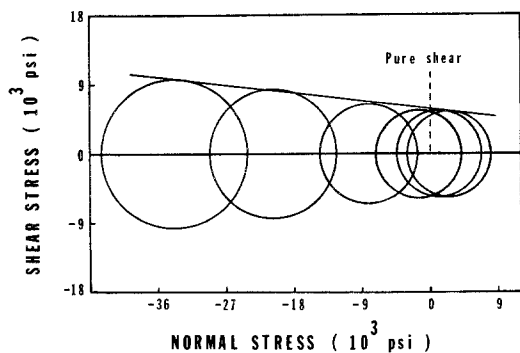


Figure 10 Mohr-circles for upper yielding of sealed specimens. The common tangent (solid line) gives the maximum shear stress; the dotted line indicates pure shear yielding.

of  $K_{max}$  and  $\alpha$  were found to be  $3.96 \times 10^7$  Pa and 0.115, respectively. The normal stress coefficient (Mohr–Coulomb) and octahedral normal stress coefficient (von Mises) were found to be quite similar.

### 3.7. Time-dependent environmental effect

In order to study the kinetic effect on the environmental stress cracking behaviour, unsealed tests in silicon oil were conducted at two strain rates at  $7 \times 10^7$  Pa. The interesting results are shown in Fig. 11. Although it is well known that the toughness of polymers increases with decreasing strain rate, at  $10\% \text{ min}^{-1}$  the sample showed ductile behaviour while at the lower strain rate of  $0.65\% \text{ min}^{-1}$

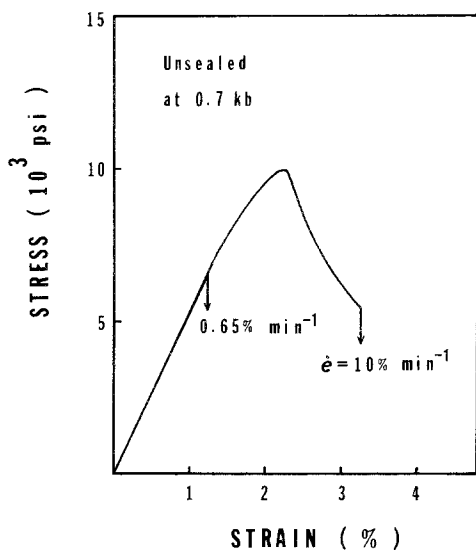


Figure 11 The effect of strain rate on the stress–strain curve of an unsealed specimen at 0.7 kbar ( $7 \times 10^7$  Pa.)

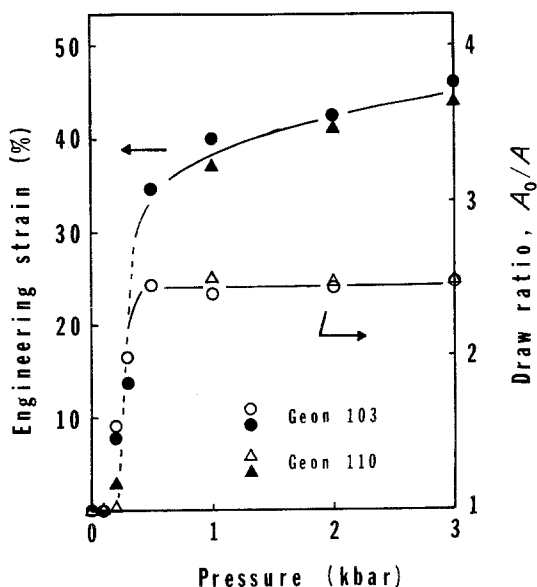


Figure 12 The ultimate engineering strain and draw ratio at various pressures.  $A_0$  and  $A$  denote the original and drawn cross-section areas, respectively.

$\text{min}^{-1}$  fracture occurred in a brittle manner. This “opposite” effect of the strain rate indicates that a certain time period is required to facilitate the penetration of silicon oil into the polymer. Subsequently, transport factors, such as the viscosity of the environmental liquid, affect the brittle-to-ductile transition behaviour [7–9].

### 3.8. Drawing process

Fig. 12 shows the ultimate draw ratio and engineering strain for sealed specimens drawn at various pressures. Samples of Geon 110 tested at  $3 \times 10^7$  and  $5 \times 10^7$  Pa failed at the unsealed threaded end of the sample after necking. This is due to the environmental stress cracking effect of silicon oil and the ultimate strain data for these samples are not included. In the post-yield region the ultimate engineering strain increases with increasing pressure, while the draw ratio reaches a maximum value of 2.5 at  $5 \times 10^7$  Pa and remains constant at higher pressures. This indicates that drawing occurs in two stages. Initially, local narrowing produces a neck. When the draw ratio on the neck reaches a maximum value, deformation proceeds by the transformation of undrawn material into the neck. Comparison of Geon 103 and Geon 110 indicates that the draw ratio in the neck does not depend on the molecular weight and therefore must be an intrinsic property of the material. On the other hand, the molecular weight does have an

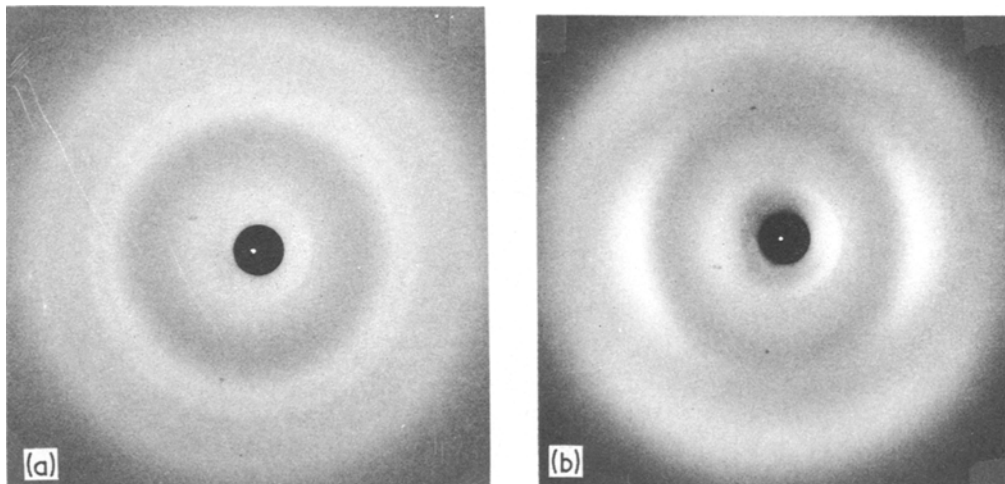


Figure 13 Wide angle X-ray diffraction patterns of (a) the unstretched sample, and (b) the sample stretched under 2.0 kbar ( $2 \times 10^8$  Pa), draw ratio is 2.45. The beam is perpendicular to the draw direction.

effect on the ultimate strain. Since failure is a localized event, occurring when the localized stress at a flaw reaches a critical condition, the lower failure strain of Geon 110 could be attributed to entanglement density or to a higher flaw density induced by the higher number of chain ends.

Fig. 13 shows the wide angle X-ray diffraction patterns of the unstretched specimen of Geon 110 and the sample drawn at  $2 \times 10^8$  Pa with draw ratio 2.5. It is noted that the molecular chains are well oriented for such a low draw ratio. In Fig.

13b, an intense equatorial reflection is observed at about 0.53 nm. This could be the overlapped (110) and (200) reflections from an oriented pseudo-crystalline structure. The azimuthal intensity distribution of this diffraction arc is shown in Fig. 14. As expected from draw ratio observations, the orientation function is essentially the same for all samples drawn at pressures above  $5 \times 10^7$  Pa. The 50% maximum intensity occurs at about  $31^\circ$ .

#### 4. Conclusions

The study on the tensile mechanical properties of PVC under high pressures enabled us to examine the yield criteria, crazing behaviour, pressure dependence of modulus, and the environmental effect due to the pressure-transmitting fluid, silicon oil, on the mechanical properties. The major conclusions from this study can be summarized as follows below.

1. A brittle-to-ductile transition is observed at a pressure between  $1 \times 10^7$  and  $2 \times 10^7$  Pa.
2. Silicon oil used as a pressure-transmitting fluid has a strong environmental stress cracking effect on the mechanical properties and the brittle-to-ductile transition of PVC under high pressure.
3. A general von Mises yield criterion is established for a multi-axial stress state.
4. As compared to PS, PVC has lower brittle-to-ductile transition pressure than PS, and shows evidence of plasticization by environmental fluid under high pressure.

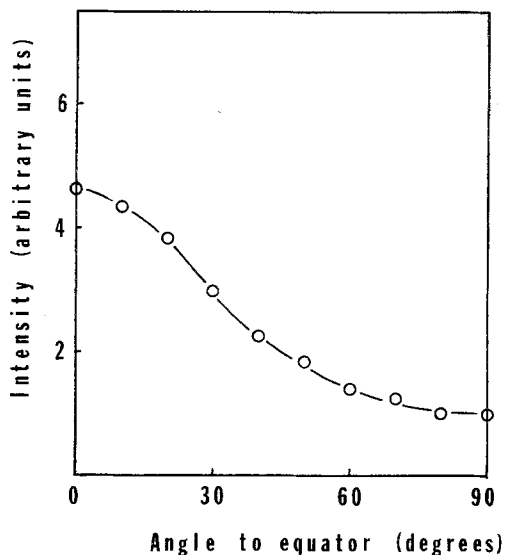


Figure 14 Azimuthal profile of the maximum intensity for the highly intense, unresolved arc at 0.53 nm.



## Acknowledgements

The authors wish to extend their thanks to Professor A. Moet, Dr C. Carman and Dr D. Rahrig for their valuable scientific contributions. This work received generous financial support from the B. F. Goodrich Company and the National Science Foundation (grant ISI 8116103) through their co-sponsorship of the Center for Applied Polymer Research.

## References

1. K. MATSUSHIGE, S. V. RADCLIFFE and E. BAER, *J. Mater. Sci.* **10** (1975) 833.
2. L. HOLLIDAY, J. MANN, G. A. POGANY, H. PUGH and D. A. GUNN, *Nature* **202** (1964) 381.
3. H. PUGH, E. F. CHANDLER, L. HOLLIDAY and J. MANN, *Polymer Eng. Sci.* **11** (1971) 463.
4. G. BIGLIONE, E. BAER and S. V. RADCLIFFE, in "Fracture 1969", edited by P. L. Pratt (Chapman and Hall, London, 1969).
5. K. MATSUSHIGE, S. V. RADCLIFFE and E. BAER, *J. Polym. Sci. Phys.* **14** (1976) 703.
6. S. K. BHATEJA and K. D. PAE, *Polym. Lett.* **10** (1972) 531.
7. K. MATSUSHIGE, E. BAER and S. V. RADCLIFFE, *J. Macromol. Sci. Phys. B* **11** (1975) 565.
8. A. MOET and E. BAER, *J. Mater. Sci.* **15** (1980) 31.
9. *Idem*, Technical Report No. 11, Case Western Reserve University, Cleveland (1980).
10. I. M. WARD, "Mechanical Properties of Solid Polymers" (John Wiley, London, 1971) p. 281.
11. A. W. CHRISTIANSEN, E. BAER and S. V. RADCLIFFE, *Phil. Mag.* **24** (1971) 451.
12. S. S. STERNSTEIN and L. ONGCHIN, *ACS Polym. Prepr.* **10** (1969) 1117.
13. S. S. STERNSTEIN and F. A. MYERS, *J. Macromol. Sci. Phys.* **B8** (1973) 539.
14. W. WHITNEY and R. D. ANDREWS, *J. Polym. Sci. C* **16** (1967) 2981.
15. P. B. BOWDEN and J. A. JUKES, *J. Mater. Sci.* **3** (1968) 183.
16. S. RABINOWITZ and I. M. WARD, *ibid.* **5** (1970) 29.
17. R. RAGHAVA, R. M. CADDELL and G. S. Y. YEH, *ibid.* **8** (1973) 225.
18. J. C. M. LI and J. B. C. WU, *ibid.* **11** (1976) 445.
19. S. S. STERNSTEIN, L. ONGCHIN and A. SILVERMAN, *Appl. Polym. Symp.* **7** (1968) 175.
20. R. J. OXBOROUGH and P. B. BOWDEN, *Phil. Mag.* **28** (1973) 547.
21. M. KITAGAWA, *J. Polym. Sci. Phys.* **14** (1976) 2095.
22. L. BEVAN, *J. Mater. Sci.* **13** (1978) 216.
23. R. A. DUCKETT, B. C. GOSWAMI, L. S. A. SMITH, I. M. WARD and A. M. ZIHLIF, *Brit. Polym. J.* **10** (1978) 11.
24. A. N. GENT, *J. Mater. Sci.* **5** (1970) 925.
25. A. MOET, I. PALLEY and E. BAER, *ACS Org. Coatings Plast. Chem.* **41** (1979) 424.
26. S. B. AINBINDER, M. G. LAKA and I. YU. MAIORS, *Polym. Mech.* **1** (1965) 50.
27. D. R. MEARS, K. D. PAE and J. A. SAUER, *J. Appl. Phys.* **40** (1969) 4229.
28. J. A. SAUER, D. R. MEARS and K. D. PAE, *Eur. Polym. J.* **6** (1970) 1015.
29. J. A. SAUER, K. D. PAE and S. K. BHATEJA, *J. Macromol. Sci. Phys.* **B8** (1973) 631.
30. K. D. PAE and J. A. SAUER, in "Engineering Solid Under Pressure; Paper presented at the Third Conference on High Pressure, Aviemore, Scotland, 1970", edited by H. L. D. Pugh (Institution of Mechanical Engineers, London, 1971).
31. D. SARDAR, S. V. RADCLIFFE and E. BAER, *Polym. Eng. Sci.* **8** (1968) 290.
32. R. W. WARFIELD, *J. Appl. Chem.* **17** (1967) 263.
33. F. MURNAGHAN, *Amer. J. Math.* **59** (1937) 235.
34. F. BIRCH, *J. Appl. Phys.* **2** (1938) 279.
35. J. M. O'REILLY, *J. Polym. Sci.* **57** (1962) 429.
36. M. BONNIN, C. M. R. DUNN and S. TURNER, *Plast. Polym.* **37** (1969) 517.
37. J. HOARE and D. HULL, *Phil. Mag.* **26** (1972) 443.
38. P. B. BOWDEN and J. A. JUKES, *J. Mater. Sci.* **7** (1972) 52.

Received 7 December 1982

and accepted 24 February 1983